The Journal of Chemical Physics

Selectivity of ion transport in narrow carbon nanotubes depends on the driving force due to drag or drive nature of their active hydration shells

Cite as: J. Chem. Phys. **154**, 104707 (2021); https://doi.org/10.1063/5.0038662
Submitted: 24 November 2020 . Accepted: 17 February 2021 . Published Online: 10 March 2021

Haiqi Gao, Jing Wang, Yuzhen Liu, Yannan Xie, Petr Král, and Ruifeng Lu

AIP Publishing

The Journal of Chemical Physics ARTICLE scitation.org/journal/jcp

Selectivity of ion transport in narrow carbon nanotubes depends on the driving force due to drag or drive nature of their active hydration shells

Cite as: J. Chem. Phys. 154, 104707 (2021); doi: 10.1063/5.0038662
Submitted: 24 November 2020 • Accepted: 17 February 2021 •
Published Online: 10 March 2021

Haiqi Gao,[1,2,3] Jing Wang,[1] Yuzhen Liu,[1,a)] Yannan Xie,[3] Petr Král,[2,4,5,6] and Ruifeng Lu[1,b)]

AFFILIATIONS

[1]Department of Applied Physics, Nanjing University of Science and Technology, Nanjing 210094, People's Republic of China
[2]Department of Chemistry, University of Illinois at Chicago, Chicago, Illinois 60607, USA
[3]Key Laboratory for Organic Electronics and Information Displays (KLOEID), Jiangsu Key Laboratory for Biosensors, Jiangsu National Synergetic Innovation Center for Advanced Materials (SICAM), Institute of Advanced Materials (IAM), Nanjing University of Posts and Telecommunications, Nanjing 210023, People's Republic of China
[4]Department of Physics, University of Illinois at Chicago, Chicago, Illinois 60607, USA
[5]Department of Pharmaceutical Sciences, University of Illinois at Chicago, Chicago, Illinois 60607, USA
[6]Department of Chemical Engineering, University of Illinois at Chicago, Chicago, Illinois 60607, USA

Note: This paper is part of the JCP Special Topic on Fluids in Nanopores.
[a)]**Email:** yzliu@njust.edu.cn
[b)]**Author to whom correspondence should be addressed:** rflu@njust.edu.cn

ABSTRACT

Molecular dynamics simulations have revealed the important roles of hydration shells of ions transported through ultrathin carbon nanotubes (CNTs). In particular, ions driven by electric fields tend to drag their hydration shells behind them, while for ions transported by pressure, their hydration shells can actively drive them. Given the different binding strengths of hydration shells to ions of different sizes, these active roles of hydration shells affect the relative entry rates and driving speeds of ions in CNTs.

I. INTRODUCTION

Selective entrance and transport of ions in nanochannels play a critical role in many applications such as cellular transport,[1] ion separation,[2–5] desalination,[6–8] and energy harvesting.[9] In these transport phenomena ions which pass through ultrasmall nanopores can be actively or passively dehydrated.[2,10–15] When the pore size is comparable to or smaller than the ionic hydration shell, some water molecules need to be stripped from the hydration shell of the ion for it to enter the channel.[16] The ion dehydration energy is usually very high. In charged, polar or polarizable nanopores, the hydration shell can be transiently stripped from ions passing the pores. In neutral nanopores, a steric exclusion of the hydrated ions usually determines the nanopore selectivity.[13,17,18] Other interactions between ions and nanopores can also affect both water and ion transport.[19]

Although different hypotheses have been proposed, there is still lack of clear understanding and consensus on the origin of ion selectivity in nanochannels.[20,21] For example, many experimental and theoretical studies predict opposite selectivity of Na^+ and K^+ ions.[2,12,22–24] For instance, Esfandiar *et al.*[10] showed in their experiment that more K^+ ions pass through the neutral angstrom-scale graphene slits than Na^+ by electric field driving. Analogously, Sint *et al.*[2] and Chen *et al.*[25] found in molecular dynamics (MD) simulations a higher rejection ratio of Na^+ than K^+ across

nanoporous graphene under the electric field driving because larger K^+ ions can more easily shed their hydration shells when passing ultrasmall nanopores. However, Song and Corry[12] and Li *et al.*[26] observed in MD simulations that the Na^+ ions have a higher transport ratio than K^+ by pressure driving through neutral CNT and nanoporous graphene, respectively. Separation and filtration of these two cations are critical in diverse applications.[23] Thus, it is indispensable to figure out the selectivity mechanism including the exact role of dehydration and other possible roles of the hydration shells.

Theoretical studies investigated the ion selectivity mainly by analyzing the ionic hydration energy[16,23] and the free energy barrier.[13,22,24,27,28] Molecular-level insights into the structural and dynamical behaviors of the ionic hydration shell are critical to elucidate ion transfer and selectivity mechanisms inside the confined nanochannels. However, very few equilibrium MD simulations have explored the dynamics of the ionic hydration shell in CNTs.[23,29]

In this work, we study selective transport of K^+ and Na^+ ions in narrow CNTs. We clarify the role of hydration shells in the selectivity of ions driven through neutral CNTs by different forces. Generally speaking, by electric field driving, the shell is lagging behind the ion (the ion is dragging the shell), while by pressure driving, the ion is lagging behind the shell (the ion is driven by the shell). The hydration shell dynamics are discussed in detail.

II. MODEL AND METHOD

Figure 1 shows the simulated system formed by CNTs embedded into two graphene slabs (4.16×4.25 nm^2) with two reservoirs on both CNT sides with a 4 nm thick salt solution along the *z* direction. Ion transport through four CNTs (55 Å long) with different effective diameters [4.6 Å, 6.8 Å, 7.3 Å, and 8.7 Å for (n,n) CNTs, n = 6–9, respectively] was studied (see Table S1 of the supplementary material). The simulation box was filled with a mixed salt solution of 4973 water molecules and 37 Na^+, 37 K^+, and 74 Cl^- ions. The ions were driven through these CNTs by the external electric field (E) or hydrostatic pressure (P). The hydrostatic pressure was obtained by applying an external force on water molecules along the *z* direction.[30] The constant force applied on each molecule is given by $F = \Delta P \cdot A/n$, where ΔP is the chosen pressure, A is the membrane area, and n is the total number of water molecules in the box.

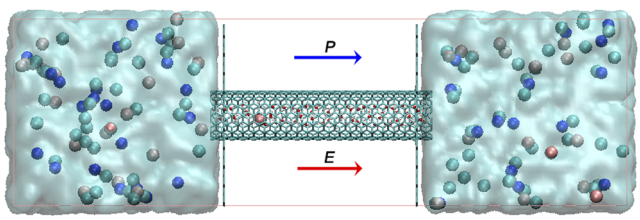

FIG. 1. The simulation system with the (7,7) CNT and K^+ (pink), Na^+ (blue), Cl^- (cyan), and water (cyan shade) molecules.

The MD simulations were performed by using Gromacs2016.3,[31] where the SPC/E[32] model is used for water. CNTs, ions, and graphene slabs are described by the Optimized Potentials for Liquid Simulations-All Atom (OPLS-AA) force field.[33] The van der Waals interactions and short range repulsions between i and j atoms are modeled by Lennard-Jones (LJ) interactions with a cutoff of 14 Å and evaluated by the combining rules, $\varepsilon_{ij} = (\varepsilon_i \varepsilon_j)^{1/2}$ and $\sigma_{ij} = (\sigma_i + \sigma_j)^{1/2}$, where ε_{ij} are the effective well depths and σ_{ij} are the minimum positions. The electrostatic interactions are evaluated by the particle-mesh Ewald method[34] with a real-space cutoff of 1.4 Å. The simulations were carried out in an NVT ensemble with periodic boundary conditions applied in the ***xyz*** direction.

Initially, the systems were energy minimized, thermalized at $T = 298$ K, and equilibrated for 100 ps in an NPT ensemble. Then, each system was independently simulated three times over 35 ns with a time step of 1 fs in an NVT ensemble. The temperature was controlled by a Nose–Hoover method with a relaxation time of 0.1 ps. Data over the last 30 ns were collected every 10 ps to calculate the ion flow. In order to gain more detailed information about the dynamics of the ionic hydration shell, extra simulations were done with frames collected every 1 ps for each system, and the time step is also 1 fs. During all the simulations, the atoms of CNTs and graphene slabs were fixed to keep the CNT pore size constant, but the ions and water molecules can move freely. The results were visualized using visual molecular dynamics.[35]

III. RESULTS AND DISCUSSION

A. Electric-field driving

Figure 2(a) shows the average ion flow through CNTs of different pore sizes driven by an electric field of $E = 1$ V/nm. In this work, the average ion flow is expressed as $I = ne/t$, where n is the total number of ions finishing the transmembrane process (entering and passing through the CNTs), t is the total time, and e is the unit charge. The simulated results reveal that more K^+ than Na^+ ions pass through CNTs, except for the (6,6) CNT. The ion flow increases with the effective pore size. For other electric fields, the ion passage rates have the same trend (see Fig. S1a of the supplementary material). The (6,6) CNT shows a complete steric exclusion of ions at an electric field of $E = 1$ V/nm. Only a few ions are monitored to pass through the (6,6) CNT driven by a much stronger E field (3 V/nm), still favoring the passage of K^+ over Na^+, which is consistent with the previous experiments in which the electric field drives ions through the interlayer space channel,[10] graphene pore,[2,36] and CNT at the angstrom scale.[37] These results are similar like in bulk water, where larger K^+ moves faster since they do not hold tightly their hydration shells.

B. Pressure driving

Different ion passage rates can also be exhibited when ions are driven by pressure through the CNT.[12] During desalination, the hydrostatic pressure (P) is the most commonly used method to filter water from a salt solution (inverse osmosis).[6,7,38] We examine the role of the hydration shell during the hydrostatic pressure-driven ion transport through CNTs. Figure 2(b) shows the ion flow through the CNT of different pore sizes under 300 MPa pressure. Clearly,

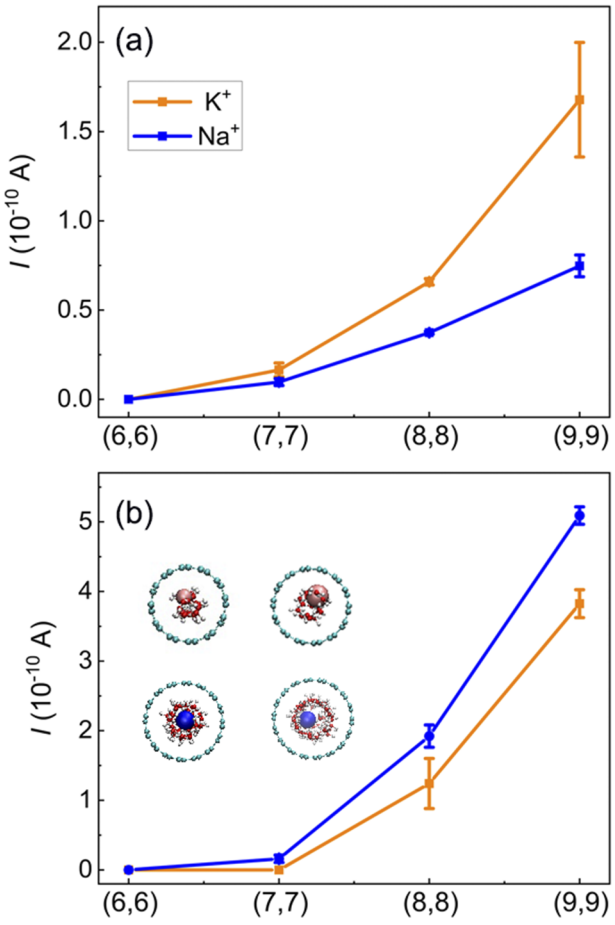

FIG. 2. Ion flows through (6,6), (7,7), (8,8), and (9,9) CNTs by (a) an electric field of E = 1.0 V/nm and (b) a pressure driving of P = 300 MPa.

no ion can pass through the narrowest (6,6) CNT even though the pressure reaches 500 MPa. Only a few Na^+ pass through the (7,7) CNT, while K^+ are still fully rejected. The ion flow increases with the increasing pore sizes. However, unlike the electric field driving, wide CNTs favor the passage of Na^+ over K^+ under hydrostatic pressure. The same behavior takes part at other pressures (see Fig. S1b of the supplementary material). Our results are consistent with previous simulations,[39] which noted that the pore radius and pressure determine which ion will permeate through CNTs.

The ion transmembrane processes could be divided into three steps: (1) ions gather nearby CNTs when driven by external forces, (2) ions are partially dehydrated to enter into narrow CNTs, and (3) ions are transported through CNTs. From our simulations, we can conclude that the type of driving force plays an important role in determining the ionic passage rates. In this work, we consider two transport modes: (i) ions tend to drag and change the hydration shell when they pass through the channel under the electric field, and (ii) ions and their shells are dragged together by pressure within CNTs. In electric field driving, the ion can often move from shell to shell by gradually exchanging water molecules. In pressure driving, the shell is pushed and carries its ion, while being less changed.

The ion–oxygen radial distribution functions [RDFs, $g(r)$] of Na^+ and K^+ inside the CNTs and bulk solution are displayed in Fig. 3. In bulk water, we can identify two peaks in $g(r)$ for both Na^+ and K^+, indicating two hydration shells formed (see Fig. S2 of the supplementary material). All the peaks of Na^+ hydration shells are smaller than those of K^+ hydration shells.[23,40] In electric field the second hydration shells almost disappear inside the (7,7) CNT, as shown in Figs. 3(a) and 3(b). It means that the second hydration shell is practically destroyed inside narrow CNTs compared to bulk. The second hydration shell is also changed and partially destroyed inside (8,8) and (9,9), while for Na^+ this shell is closer to the ion due to the applied field. Under hydrostatic pressure, the hydration shell peaks of Na^+ and K^+ inside (8,8) and (9,9) CNTs are more pronounced compared to the bulk phase. Therefore, the hydration shells are under pressure not shifted and crashed on the ions like in the presence of strong electric fields.

Partial dehydration of the first shell is the origin of the ion passage rates across the neutral pore.[12,13,17,22] The role of

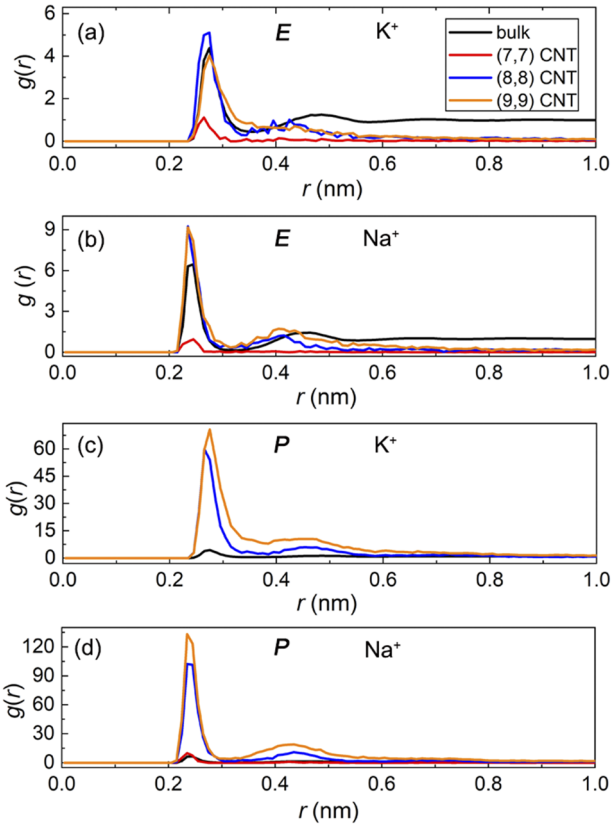

FIG. 3. The K^+–O and Na^+–O RDFs in the bulk phase and inside CNT channels under the electric field (1 V/nm) for K^+ (a) and Na^+ (b) and under pressure (300 MPa) for K^+ (c) and Na^+ (d).

TABLE I. Average number of water molecules (N_c, coordination number) around the first and second hydration shells for K^+ and Na^+ inside CNTs [counted when ions permeate through CNTs by the electric field (*E*) and pressure driving (*P*)] and bulk solution with errors in the parentheses.

	K^+				Na^+			
	The first shell		The second shell		The first shell		The second shell	
CNTs	*E*	*P*	*E*	*P*	*E*	*P*	*E*	*P*
(7,7)	4.6(±0.3)		9.5(±0.8)		4.5(±0.2)	4.5(±0.1)	9.5(±0.6)	9.2(±0.4)
(8,8)	5.4(±0.5)	5.7(±0.2)	12.9(±1.2)	11.8(±0.9)	6.1(±0.4)	5.3(±0.3)	13.3(±0.8)	11.7(±0.7)
(9,9)	8.6(±0.6)	6.4(±0.4)	19.5(±2.1)	15.7(±1.4)	5.6(±0.3)	4.7(±0.2)	17.7(±1.8)	14.6(±1.1)
Bulk	5.9(±0.7)		20.9(±2.5)		4.8(±0.4)		18.4(±1.6)	

dehydration of the second hydration shell in ion selectivity is usually ignored for K^+ and Na^+ separation.[12] The energy barrier of K^+/Na^+ at the entrance of wider channels such as the (8,8) or (9,9) CNT is simply attributed to the geometric change in the solvation shell.[12,23] It was found that the dehydration of the second hydration shell also contributes to the energy barrier for Mg^+/Li^+ entering into nanochannels.[41] Here, we discuss the dehydration processes of two hydration shells for the two above-mentioned modes. The ionic hydration radii were obtained according to the RDF of water molecules around the ion in the bulk solution (see Fig. S2 of the supplementary material). The first and second shell radii were about 0.355 nm and 0.575 nm for K^+ and 0.325 nm and 0.55 nm for Na^+, respectively, which agree well with previous works.[23,25,40,42,43] The shell radii of ions inside the CNT are considered to be the same as the bulk solution in this work.[23] The water molecules will be counted when the distance between the oxygen atom in the water molecule and the ion is less than the first and second shell radii as the first coordination number (N_c) and second coordination number,[43] respectively.

The average numbers of water molecules in the first hydration shell and the second hydration shell in the bulk solution and inside CNTs are shown in Table I. The ion coordination number

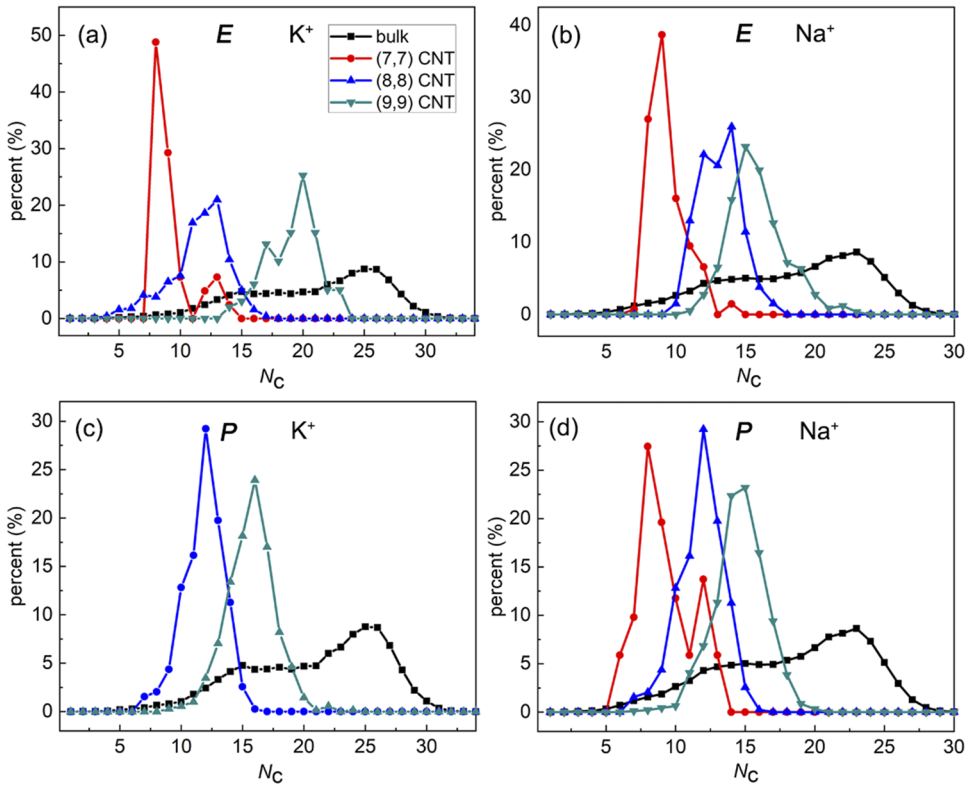

FIG. 4. The coordination number (N_c) distributions of the second hydration shells in the bulk solution and inside CNTs under an electric field of 1 V/nm for K^+ (a) and Na^+ (b) and under 300 MPa for K^+ (c) and Na^+ (d).

fluctuates due to the dynamic changes in the hydration shell. In bulk solution, the first shell coordination numbers of K^+ and Na^+ are distributed in the range of 5–7 and 4–6 with average values of 5.858 and 4.809, respectively (see Fig. S3 of the supplementary material and Table I). These coordination numbers agree well with previous experiments and simulations.[25,40] Inside the (7,7) CNT, N_c of the first hydration shell is 4–5 for both Na^+ and K^+ ions under the two driving forces, as shown in Fig. S3 of the supplementary material. However, the coordination numbers are obviously higher than those in the bulk solution for the K^+ ion inside the (9,9) CNT and the Na^+ ion inside the (8,8) CNT, especially for electric field driving. The confinement effect on the hydration shell inside CNTs can explain this behavior.[12] The dehydration of the first shell of Na^+ and K^+ only occurs when entering the (7,7) CNT, which is consistent with previous equilibrium MD and non-equilibrium MD simulation results.[12,23]

Table I shows that the average N_c of the second hydration shell is reduced for each model except for K^+ ions inside the (9,9) CNT by electric field driving. Figure 4 shows that in the bulk solution, the N_c profiles of the second hydration shells for both K^+ and Na^+ distribute broadly with peaks appeared at 25–26 and 22–24, respectively, but more concentrated in CNTs. From the N_c distribution, we can see that the peak of the second hydration shell inside the (9,9) CNT is located at 20 by electric driving, indicating that water molecules can be still stripped from the second shell. In addition, by comparing two driving methods, we find that more water molecules will be stripped from the hydration shell by pressure driving (Table I). Such as the case inside the (8,8) CNT, about eight and seven water molecules will be stripped from the second shell by E driving, whereas nine and eight water molecules will be lost from the second shell under pressure, respectively, for K^+ and Na^+ ions. Although more water molecules are stripped from the hydration shell of K^+ than that of Na^+ under both driving methods, the ions passage rates is quite different when entering the neutral CNTs. The free energy barrier calculated by previous work can be ascribed to dehydration of the first and second hydration shells, not merely to the first dehydration.[12,44]

The dehydration process of the second shell for the K^+ ion passing through the (7,7) CNT driven by the electric field is shown in Fig. 5. While N_c keeps fluctuating in a certain range in the bulk solution, a drastic water shedding from the second shell can be found at the entrance of the narrower channel. A similar dehydration process can be observed for K^+ and Na^+ permeating through other size CNTs under pressure or electric field (see Fig. S4 of the supplementary material). Partial dehydration in the first shell only occurs at the entrance of the (7,7) CNT (see Fig. S5 of the supplementary material). Different from water molecules in bulk, water confined in nanoscale channels can form various water structures.[45,46] Similar to the previous studies, the water conformation in CNTs in this work is also changed from disordered to ordered structures under the electric field.[47] The ordered helical structures can be found in (7,7), (8,8), and (9,9) CNTs, while the ordered single-chain structure can be observed in the (6,6) CNT (see Fig. S6 of the supplementary material).

In order to better understand the two proposed modes of ion transport through CNTs, the average residence time of water molecules in the hydration shell of K^+ and Na^+ in the bulk solution and inside CNTs is shown in Fig. 6. More detailed distribution

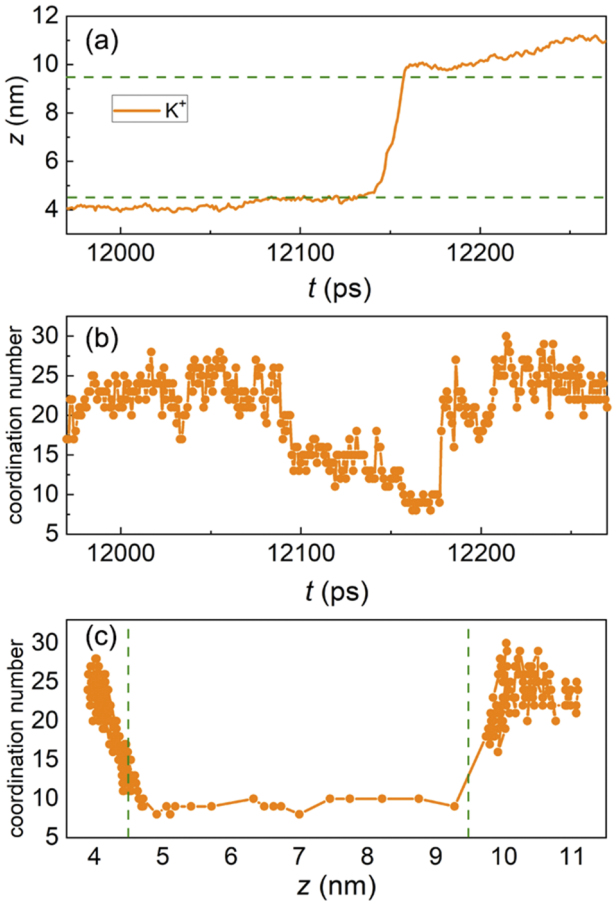

FIG. 5. (a) A trajectory of K^+ passing through the (7,7) CNT along the ***z*** direction under an electric field of 1 V/nm. (b) The second coordination number of K^+ vs time when entering the (7,7) CNT. (c) The second coordination number of K^+ along the +z direction when entering the (7,7) CNT.

profiles of residence time for K^+ and Na^+ in the bulk solution without external driving force are provided in Fig. S7 of the supplementary material. The residence time of water molecules in the hydration shell is obtained by integrating the time correlation functions of 1 or 0 if the water is in the first shell or not.[48,49] It is well known that the water in the hydrated shell is relatively stable, and the water molecules constantly exchange between the ionic hydration shell and the bulk solution. The exchange of water molecules between those formed hydration shells and the surrounding bulk water is very frequent, especially for K^+, about half of the water molecules stay in the first shell with a residence time of less than 2 ps (see Fig. S7 of the supplementary material). The measured average residence time in this work is about 4.5 ps for the K^+ ion and 14.3 for the Na^+ ion in the bulk solution, which are consistent with previously reported values.[48,49] It can be reflected that the hydrated water is sufficiently tightly held around the Na^+ ion than the K^+ ion.

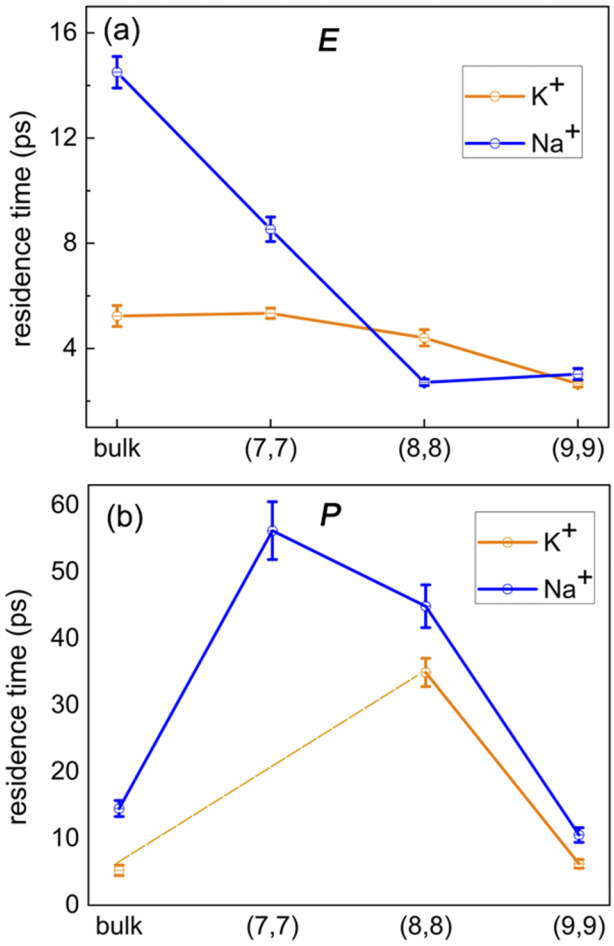

FIG. 6. Residence time of water in the bulk solution and inside CNTs under the electric field (1 V/nm) (a) and (b) pressure (300 MPa).

The hydration shell is more stable inside CNTs at the quasi-steady state,[48] but the behavior of the water structure when ions permeate through CNTs by external forces has not been studied yet. Figure 6(a) shows the average residence time of water molecules in the hydration shell of K^+ and Na^+ ions inside CNTs by the electric field driving. The average residence time inside the CNT is less than that in the bulk phase and inversely proportional to the pore size. Thus, contrary to the quasi-steady state, the hydration shell of the ion inside the CNT is weaker than that in the bulk phase by electric field driving, and it becomes weaker as the pore size increases. However, under pressure, the narrower channel corresponds to the more stable water structure [Fig. 6(b)]. The average residence time of water molecules in the hydration shell of the Na^+ ion inside the (7,7) CNT is of up to 56 ps, much larger than 14.5 ps in the bulk solution. The distinct exchange frequency between the water structure and the bulk solution under two driving methods reveals the different ion transport modes. Moreover, the evolution process of water molecules around the first shell is provided in Fig. S8 of the supplementary material, from which the two transport modes can be directly observed. Ions tend to escape from the hydration shell, and then, a new hydration shell is formed around the ion to pass through the channel by electric field driving. Thus, the average residence time of water molecules in the hydration shell of the ion inside the CNT is less than that in the bulk phase [Fig. 6(b)]. However, the ion will be dragged by hydrated water to pass through CNTs by pressure driving, so the hydration shell becomes more and more stable inside CNTs [Fig. 6(b)].

We believe that the above-mentioned three steps in ion transmembrane process together affect the ions selectivity. The numbers of K^+ and Na^+ ions along the z direction of the (9,9) CNT are shown in Fig. 7. For the first transport mode by electric field driving, more K^+ ions gather around the entrance of the CNT [Fig. 7(a)]. In

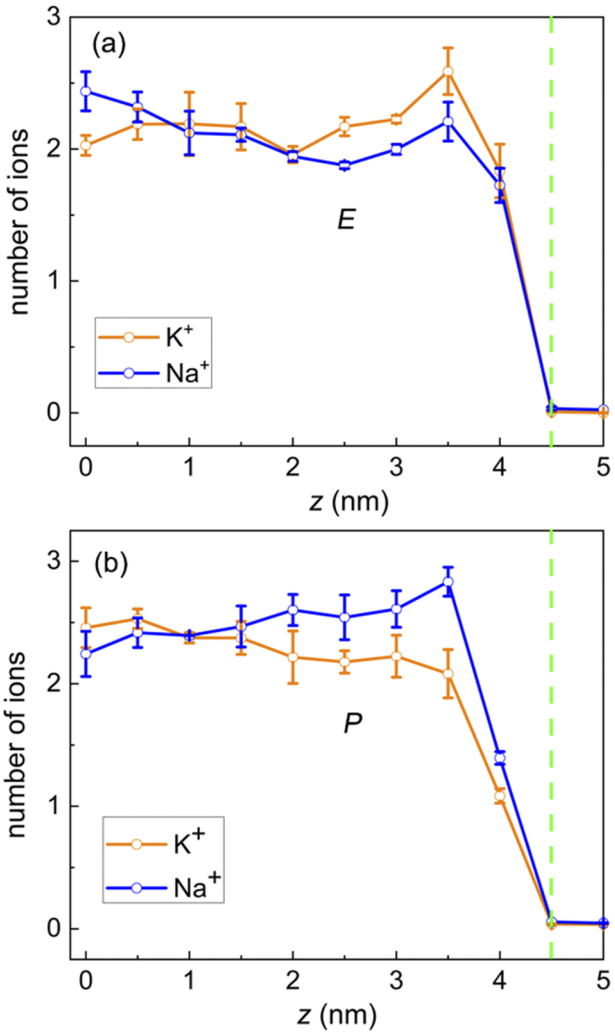

FIG. 7. The numbers of Na^+ and K^+ ions along the z direction for the (9,9) CNT by (a) electric field driving and (b) pressure driving. The green line represents the entrance of the CNT.

TABLE II. Average transport time of ions to enter CNTs with errors in the parentheses.

	Electric field driving			Pressure driving		
	(7,7) CNT	(8,8) CNT	(9,9) CNT	(7,7) CNT	(8,8) CNT	(9,9) CNT
K^+ (ps)	150(±2)	148(±1)	73(±3)	...	88(±5)	59(±4)
Na^+ (ps)	160(±3)	166(±2)	133(±5)	463(±19)	122(±8)	68(±3)

addition, K^+ ions can easily break the continuously formed weaker hydration shell [Figs. 3(a), 3(b), and 6(a)]. Therefore, K^+ will spend less time than Na^+ to enter and pass through CNTs by electric field driving (see Table II and Fig. S9 of the supplementary material). The ice-like water structure and confinement effect make the hydration shell of the K^+ ion more stable than Na^+ inside the (8,8) CNT [Fig. 6(a)].[12] Therefore, inside the (8,8) CNT, the K^+ ion is harder to break the hydration shell, leading to a slower transport through the channel (Table III). However, the first and second steps play the dominant role in ion selectivity under the electric field. More K^+ ions will gather around the entrance of CNTs, and they easily escape from the hydration shell by dehydration and fast transport through the channel. Therefore, by electric field driving, the CNT can achieve K^+ separation from the Na^+/K^+ mixed solution [Fig. 2(a)].

In contrast, for pressure driving, more Na^+ ions dragged by tightly hydrated water gather around CNTs than K^+ [Fig. 7(b)]. The hydration energy in the first shell is much larger than that in the second shell, which makes the dehydration of the first hydration shell much harder than that of the second shell. On average 1.3 and 0.3 water molecules need to be stripped from the first hydration shells of K^+ and Na^+ when they enter the narrower (7,7) CNT, respectively (see Table I and Fig. S3 of the supplementary material). No ions can pass through the narrowest (6,6) CNT even under a higher external force (500 MPa or 3 V/nm) due to the fact that more water molecules need to shed from the first hydration shell. The Na^+ ions with less water dehydrated from the first shell can be strongly dragged by tightly hydrated water to slowly enter the (7,7) CNT [Fig. 2(b) and Table II]. For K^+ ions, the weaker hydration shell cannot supply enough energy to peel off about 1.3 water molecules from the first hydration shell. Only Na^+ ions are monitored to enter the confined (7,7) CNT. For the (8,8) and (9,9) CNTs, only the dehydration of the second hydration shell (Fig. 4) and the change in the hydrated structure are the origin of the free energy barrier when ions enter the wider CNTs. The K^+ ion with the weaker second hydration shell can easily change its water structure and peel off water molecules from the second shell. Thus, K^+ ions spend less time than Na^+ to enter the wider channel (Table II). After entering the wider CNTs, the two cations spend similar time to pass through CNTs, which is different from the case of electric field driving (Table III). We know that when the first hydration shell is not dehydrated, the first step plays a major role in ion selectivity. By pressure driving, more Na^+ ions enter (high entry rate) the wider CNTs.

Moreover, the effect of temperature on ion transport through CNTs under two external driving forces is explored. Figure 8 for the (8,8) CNT shows that the ion flow is proportional to the temperature by the two driving modes. In addition, the ion selectivity is kept constant at different temperatures in our simulation. The orientation of water inside the hydration shell of the cation is sensitive to the temperature, and a high temperature makes the hydration shells more unstable.[50] Thus, with the temperature increase, the hydration energy will decrease,[51] and the water molecules are more easily stripped from the hydration structure to enter the channel, leading to an enhanced ion flow. The ion transport through the nanochannel would be affected by the used force field parameters of ion and water models.[52,53] In this work, the TIP3P water model was also considered, and all other particles were still described by the Optimized Potentials for Liquid Simulations-All Atom (OPLS-AA) force field. The average ion flows through the CNTs driven by an electric field of 1 V/nm and a pressure of 300 MPa are plotted in Fig. S10 of the supplementary material, which show some differences for both Na^+ and K^+ compared to the results from the SPC/E model (Fig. 8). However, under the two external forces, the selective ion transport is consistent for the two water models.

To check the effect of the ion force field on ion selectivity, the CHARMM27[54] force field was used to simulate the (9,9) CNT system. More specifically, we assigned $\sigma = 0.355$ and $\varepsilon = 0.292\,88$ without considering partial atomic charge, the default CHARMM27

TABLE III. Average transport time of ions to pass through CNTs with errors in the parentheses.

	Electric field driving			Pressure driving		
	(7,7) CNT	(8,8) CNT	(9,9) CNT	(7,7) CNT	(8,8) CNT	(9,9) CNT
K^+	14(±2)	31(±5)	12(±3)	...	161(±10)	131(±7)
Na^+	20(±1)	15(±0.5)	48(±6)	122(±4)	162(±9)	131(±5)

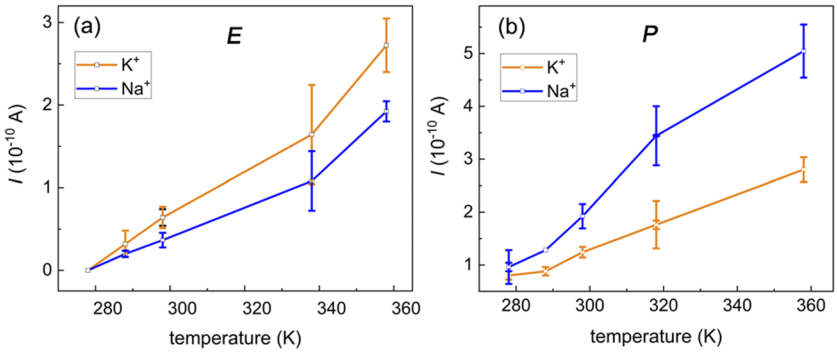

FIG. 8. Ion flow inside the (8,8) CNT at different temperatures (278 K, 288 K, 298 K, 328 K, and 348 K) under (a) electric field (1 V/nm) and (b) pressure (300 MPa).

parameters, and the SPC/E model to carbon atoms, ions, and water molecules, respectively. The numbers of K^+ and Na^+ passing through the (9,9) CNT under an electric field of 1.0 V/nm and a pressure of 300 MPa are shown in Fig. S11 of the supplementary material. Although the simulated results are different from those by the OPLS-AA force field, the ion selectivity will be unchanged, i.e., no matter what force field parameters or models are employed, more Na^+ ions pass through CNTs when driven by pressure, whereas K^+ ions pass through the same channel more easily driven by the electric field.

IV. CONCLUSION

In summary, using molecular dynamics simulations, the effect of driving force on ionic selectivity, transport, and the dehydration process of K^+ and Na^+ passing through the angstrom-scale channel was explored. We proposed two transport modes for ions passing through CNTs and found that driving force and the hydration shell together determine the ion passage rates. Ions tend to escape from the hydration shell to enter and pass through CNTs by electric field driving but will be dragged by water molecules to pass through CNTs under pressure. Thus, the weaker hydration shells of K^+ ions are easier to shed their hydrated water to enter and pass through CNTs under the electric field. However, with the tighter (smaller radii) ionic hydration shells, Na^+ ions will lose less water to pass through the narrowest channel by pressure driving, while more Na^+ ions gather and enter the wider CNTs by tightly hydrated water dragging. The findings and insights obtained in this work can greatly enrich our understanding of ion dehydration, transport, and selectivity.

SUPPLEMENTARY MATERIAL

See the supplementary material for more information on pore parameters and additional simulation results of the studied CNTs.

ACKNOWLEDGMENTS

This research was financially supported by the NSF of China (Grant No. 51872142) and the Natural Science Foundation of Jiangsu Province (Grant No. BK20170032).

DATA AVAILABILITY

The data that support the findings of this study are available from the corresponding author upon reasonable request.

REFERENCES

[1] M. C. Sanguinetti, M. E. Curran, A. Zou, J. Shen, P. S. Specter, D. L. Atkinson, and M. T. Keating, Nature **384**, 80 (1996).
[2] K. Sint, B. Wang, and P. Král, J. Am. Chem. Soc. **130**, 16448 (2008).
[3] D. A. Doyle, J. Morais Cabral, R. A. Pfuetzner, A. Kuo, J. M. Gulbis, S. L. Cohen, B. T. Chait, and R. MacKinnon, Science **280**, 69 (1998).
[4] Z. He, J. Zhou, X. Lu, and B. Corry, ACS Nano **7**, 10148 (2013).
[5] S. Zhao, J. Xue, and W. Kang, J. Chem. Phys. **139**, 114702 (2013).
[6] K. M. Gupta, Z. Qiao, K. Zhang, and J. Jiang, ACS Appl. Mater. Interfaces **8**, 13392 (2016).
[7] Q. Shi, H. Gao, Y. Zhang, Z. Meng, D. Rao, J. Su, Y. Liu, Y. Wang, and R. Lu, Carbon **136**, 21 (2018).
[8] Y. Wang, Z. He, K. M. Gupta, Q. Shi, and R. Lu, Carbon **116**, 120 (2017).
[9] A. Siria, P. Poncharal, A.-L. Biance, R. Fulcrand, X. Blase, S. T. Purcell, and L. Bocquet, Nature **494**, 455 (2013).
[10] A. Esfandiar, B. Radha, F. C. Wang, Q. Yang, S. Hu, S. Garaj, R. R. Nair, A. K. Geim, and K. Gopinadhan, Science **358**, 511 (2017).
[11] K. Gopinadhan, S. Hu, A. Esfandiar, M. Lozada-Hidalgo, F. C. Wang, Q. Yang, A. V. Tyurnina, A. Keerthi, B. Radha, and A. K. Geim, Science **363**, 145 (2019).
[12] C. Song and B. Corry, J. Phys. Chem. B **113**, 7642 (2009).
[13] S. Sahu, M. Di Ventra, and M. Zwolak, Nano Lett. **17**, 4719 (2017).
[14] R. Bhadauria and N. R. Aluru, J. Chem. Phys. **147**, 214105 (2017).
[15] L. Yang and S. Garde, J. Chem. Phys. **126**, 084706 (2007).
[16] J. Abraham, K. S. Vasu, C. D. Williams, K. Gopinadhan, Y. Su, C. T. Cherian, J. Dix, E. Prestat, S. J. Haigh, I. V. Grigorieva, P. Carbone, A. K. Geim, and R. R. Nair, Nat. Nanotechnol. **12**, 546 (2017).
[17] L. A. Richards, A. I. Schäfer, B. S. Richards, and B. Corry, Small **8**, 1701 (2012).
[18] Y. Fu, S. Su, N. Zhang, Y. Wang, X. Guo, and J. Xue, ACS Appl. Mater. Interfaces **12**, 24281 (2010).
[19] J. Liu, G. Shi, P. Guo, J. Yang, and H. Fang, Phys. Rev. Lett. **115**, 164502 (2015).
[20] M. I. Walker, K. Ubych, V. Saraswat, E. A. Chalklen, P. Braeuninger-Weimer, S. Caneva, R. S. Weatherup, S. Hofmann, and U. F. Keyser, ACS Nano **11**, 1340 (2017).
[21] B. Corry, MRS Bull. **42**, 306 (2017).
[22] Y. Yu, J. Fan, J. Xia, Y. Zhu, H. Wu, and F. Wang, Nanoscale **11**, 8449 (2019).
[23] Q. Shao, J. Zhou, L. Lu, X. Lu, Y. Zhu, and S. Jiang, Nano Lett. **9**, 989 (2009).
[24] Y. Yan, W. Li, and P. Král, Nano Lett. **17**, 6742 (2017).

[25]Y. Chen, Y. Zhu, Y. Ruan, N. Zhao, W. Liu, W. Zhuang, and X. Lu, Carbon **144**, 32 (2019).
[26]K. Li, Y. Tao, Z. Li, J. Sha, and Y. Chen, Nanotechnology **29**, 035402 (2018).
[27]Y. Kang, Z. Zhang, H. Shi, J. Zhang, L. Liang, Q. Wang, H. Ågren, and Y. Tu, Nanoscale **6**, 10666 (2014).
[28]W. Li, Y. Yang, J. K. Weber, G. Zhang, and R. Zhou, ACS Nano **10**, 1829 (2016).
[29]K. Zhou and Z. Xu, ACS Appl. Mater. Interfaces **10**, 27801 (2018).
[30]F. Zhu, E. Tajkhorshid, and K. Schulten, Biophys. J. **83**, 154 (2002).
[31]M. J. Abraham, T. Murtola, R. Schulz, S. Páll, J. C. Smith, B. Hess, and E. Lindahl, SoftwareX **1-2**, 19 (2015).
[32]W. L. Jorgensen, J. Chandrasekhar, J. D. Madura, R. W. Impey, and M. L. Klein, J. Chem. Phys. **79**, 926 (1983).
[33]W. L. Jorgensen, D. S. Maxwell, and J. Tirado-Rives, J. Am. Chem. Soc. **118**, 11225 (1996).
[34]U. Essmann, L. Perera, M. L. Berkowitz, T. Darden, H. Lee, and L. G. Pedersen, J. Chem. Phys. **103**, 8577 (1995).
[35]W. Humphrey, A. Dalke, and K. Schulten, J. Mol. Graphics **14**, 33 (1996).
[36]R. C. Rollings, A. T. Kuan, and J. A. Golovchenko, Nat. Commun. **7**, 11408 (2016).
[37]W. Choi, Z. W. Ulissi, S. F. Shimizu, D. O. Bellisario, M. D. Ellison, and M. S. Strano, Nat. Commun. **4**, 2397 (2013).
[38]H. Gao, Q. Shi, D. Rao, Y. Zhang, J. Su, Y. Liu, Y. Wang, K. Deng, and R. Lu, J. Phys. Chem. C **121**, 22105 (2017).
[39]B. Corry, J. Phys. Chem. B **112**, 1427 (2008).
[40]J. Zhou, X. Lu, Y. Wang, and J. Shi, Fluid Phase Equilib. **194-197**, 257 (2002).
[41]Y. Ruan, Y. Zhu, Y. Zhang, Q. Gao, X. Lu, and L. Lu, Langmuir **32**, 13778 (2016).
[42]E. Rigo, Z. Dong, J. H. Park, E. Kennedy, M. Hokmabadi, L. Almonte-Garcia, L. Ding, N. Aluru, and G. Timp, Nat. Commun. **10**, 2382 (2019).
[43]G. Mogami, M. Suzuki, and N. Matubayasi, J. Phys. Chem. B **120**, 1813 (2016).
[44]Y. Zhu, Y. Ruan, Y. Zhang, Y. Chen, X. Lu, and L. Lu, Langmuir **33**, 9201 (2017).
[45]Z. Qian, Z. Fu, and G. Wei, J. Chem. Phys. **140**, 154508 (2014).
[46]Z. Fu, Y. Luo, J. Ma, and G. Wei, J. Chem. Phys. **134**, 154507 (2011).
[47]Winarto, D. Takaiwa, E. Yamamoto, and K. Yasuoka, J. Chem. Phys. **142**, 124701 (2015).
[48]H. Liu, S. Murad, and C. J. Jameson, J. Chem. Phys. **125**, 084713 (2006).
[49]R. W. Impey, P. A. Madden, and I. R. McDonald, J. Phys. Chem. **87**, 5071 (1983).
[50]Q. Shao, L. Huang, J. Zhou, L. Lu, L. Zhang, X. Lu, S. Jiang, K. E. Gubbins, and W. Shen, Phys. Chem. Chem. Phys. **10**, 1896 (2008).
[51]J. Carlsson and J. Åqvist, J. Phys. Chem. B **113**, 10255 (2009).
[52]L. Liu and G. N. Patey, J. Chem. Phys. **146**, 074502 (2017).
[53]I. S. Joung and T. E. Cheatham III, J. Phys. Chem. B **112**, 9020 (2008).
[54]A. D. MacKerell, D. Bashford, M. Bellott, R. L. Dunbrack, J. D. Evanseck, M. J. Field, S. Fischer, J. Gao, H. Guo, S. Ha, D. Joseph-McCarthy, L. Kuchnir, K. Kuczera, F. T. K. Lau, C. Mattos, S. Michnick, T. Ngo, D. T. Nguyen, B. Prodhom, W. E. Reiher, B. Roux, M. Schlenkrich, J. C. Smith, R. Stote, J. Straub, M. Watanabe, J. Wiórkiewicz-Kuczera, D. Yin, and M. Karplus, J. Phys. Chem. B **102**, 3586 (1998).